Synthesis and Characterization of InAs/InP and InAs/CdSe Core/Shell Nanocrystals**

Yun-Wei Cao and Uri Banin*

Semiconductor nanocrystals have unique size-dependent optical properties governed by the quantum confinement effect.[1,2] The optical and electronic properties can also be controlled by fabricating advanced core/shell nanocrystal structures, where a shell of a higher band gap semiconductor is grown on the core, yielding superior surface passivation.[3–5] Previous work has primarily focused on II – VI semiconductor core/shell nanocrystals, for example CdSe/CdS and CdSe/ZnS.[4, 5] Significant enhancement of the emission quantum yield, and increased stability against oxidation compared to the cores, were observed. These improved nanocrystals have been used as a novel type of fluorescence markers in biological applications, with marked advantages over the traditional fluorescent dyes.[6] Here we report on the synthesis and properties of novel core/shell nanocrystals with InAs cores. The band gap of InAs nanocrystals is size tunable through the near IR spectral region, where the selection of dyes is poor and their stability is low. These core/shell nanocrystals may be useful in future applications as biological fluorescent markers in the near IR spectral region.

The enhancement of the fluorescence quantum yield in core/shell nanocrystals is based on confinement of the carrier wavefunctions to the core region. In bulk InAs, the electron effective mass is substantially smaller than in CdSe ($0.024\ m_e$ versus $0.11\ m_e$, where m_e = mass electron). As a result, the confinement of the electron wavefunction to the core region can be expected to be more problematic in InAs cores. Therefore, in this core/shell system, the quality of the outer surface may play an important role in determining the fluorescence quantum yield. We examine this issue by growing two types of shells on InAs cores: InP and CdSe. The conduction band offset between InAs and these two shell materials is nearly identical,[7] making the comparison of their properties particularly interesting.

We developed a high-temperature route to grow core/shell nanocrystals with InAs cores. Previously, a low-temperature route was used to prepare InAs/CdS core/shells in pyridine and benzylamine.[8] The high-temperature route (260 °C) is necessary here to overcome the large reaction barriers for the decomposition of InP and CdSe precursors, and is also advantageous in achieving higher crystallinity of the core/shell nanocrystals. The difficulty in using high temperature in the shell growth lies in Ostwald ripening of the nanocrystals, which leads to broadening of the size distribution.[1] For CdSe cores, ripening is fast and this limits the usable growth temperature of the shells in this case.[5] In contrast, we found that for the InAs cores, the rate of ripening is slow even at high temperature. Ripening should also be avoided during shell growth. For this we need to use high concentration of shell precursors. On the other hand, we need to prevent new nucleation of nanocrystals of the shell material, which is favorable at high concentration. By exploring the effects of core concentration, shell precursors concentration, and rate of precursor addition, we optimized the conditions for shell growth which do not yield substantial nucleation of nanocrystals of the shell semiconductor, while still minimizing the Ostwald ripening process.

Figure 1 presents the evolution of the absorption spectrum upon growth of an InP shell on InAs cores with radius of 17 Å. The shell growth is accompanied by a red shift of the spectrum, while its overall shape is nearly maintained

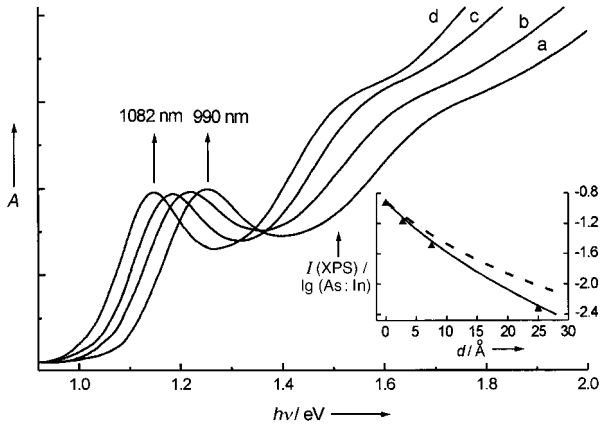

Figure 1. Absorption spectra of InAs core and InAs/InP core/shell nanocrystals during shell growth. The spectra were obtained for aliquots extracted 2 min after the injections of the InP stock solution. a) core with 17 Å in radius, core/shells with shell thickness in number of monolayers: b) 0.7, c) 1.4, d) 2.2. Insert: XPS intensity ratio of peak As_{3d} to $In_{3d5/2}$ peak (logarithmic scale), versus shell thickness *d*. Note the good agreement between the experimental data points (triangles), and a simulation of the expected ratio for a spherical core/shell structure (solid line). Also shown, is the simulated ratio for a spherical alloy structure (dashed line). The following photoelectron escape depths (λ) under $Al_{K\alpha}$ radiation (1486.6 eV) were used in the simulations: For InAs core: As_{3d}: 24.8 Å, $In_{3d5/2}$: 19.2 Å, for InP shell, As_{3d}: 24 Å, $In_{3d5/2}$: 18.6 Å.[9]

indicating that the good size distribution is preserved. Compared to the original cores, the fluorescence quantum yield in this case is substantially lowered, by a factor of 8. The systematic red shift of the band gap with the shell growth results from the extension of the carrier wavefunction into the shell region. In the case of alloy formation, a blue shift is expected.[4] Additional direct proof for the growth of the shells was provided by X-ray photoelectron spectroscopy (XPS). In the insert of Figure 1, we present the ratio of the measured intensity of the $In_{3d5/2}$ to As_{3d} peaks versus shell thickness (triangles). Upon shell growth, the photoelectron signal of As is substantially quenched because of the reduced

[*] Dr. U. Banin, Dr. Y. W. Cao
Department of Physical Chemistry
and The Farkas Center for Light-Induced Processes
The Hebrew University of Jerusalem, Jerusalem 91904 (Israel).
Fax: (972) 2-561-8033
E-mail: Banin@chem.ch.huji.ac.il

[**] This research was supported in part by a grant from the Israel Academy of Sciences and Humanities, and by a grant from the Binational US-Israel Science Foundation. The Farkas Center for Light-Induced Processes is supported by the Minerva Gesellschaft für Forschung of the German Ministry for Research and Technology (BMFT). We thank Dr. Victor Soloviev for technical assistance in the fluorescence measurements. Y.W.C. thanks the Golda Meir Foundation for a postdoctoral fellowship. U.B. thanks the Israeli Board of Higher Education for an Alon fellowship.

  1433-7851/99/3824-3692 $ 17.50+.50/0

escape probability through the InP shells. Due to the similarity between the size of the nanocrystals and the photoelectron escape depths (λ, values given in caption of Figure 1), we use the integral $\int e^{-z/\lambda} dz$ to correct the sensitivity factors of XPS peaks.[9, 10] The solid line is the calculated intensity ratio under the assumption of a core/shell spherical structure, and good agreement with the experimental data is observed.

Figure 2 presents the evolution of the absorption and emission spectra upon growth of a CdSe shell on another fraction of the same InAs cores. As in the InP case, we observe a red

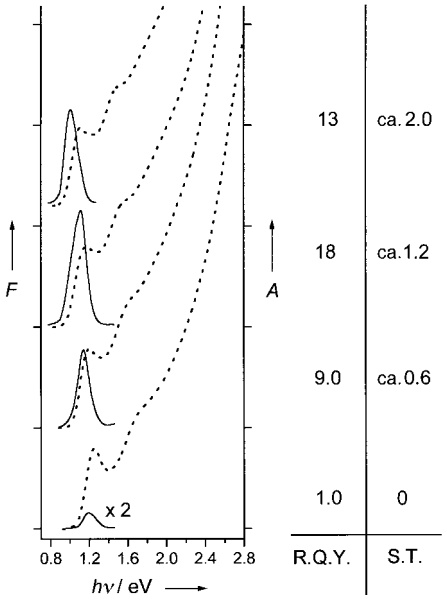

Figure 2. Absorption (dotted lines) and fluorescence (solid lines) spectra of InAs/CdSe core/shell nanocrystals. The core radius is 17 Å. The shell thickness (ST), and the relative fluorescence quantum yield (RQY), are indicated on the right side.

shift of the band gap with shell growth. But in this case, as can be seen in the figure, the fluorescence quantum yield is substantially enhanced as compared to the fresh core, up to a maximum of an 18-fold increase. The quantum yield of these InAs/CdSe core/shells was directly compared with the yield of the laser dye IR140,[11] using 826 nm excitation, and was found to be two times larger (absolute yield of 20%). To study the growth of the core/shell nanocrystals, we also used high-resolution transmission electron microscopy (HRTEM). Figure 3 shows HRTEM images of a single InAs core nanocrystal (18 Å radius, frame A), and of an InAs/CdSe core/shell nanocrystal (33 Å radius, frame B). In both nanocrystals, the zinc blende structure is observed as viewed along the [110] zone axis.

To further characterize the core/shell structures, we used powder X-ray diffraction (XRD). Figure 4 compares the diffraction patterns of InAs cores with InAs/InP and InAs/CdSe core/shells. The positions of the peaks of the InAs cores (dotted line) match those of the bulk InAs zinc blende peaks, consistent with the HRTEM images. The peaks are broadened because of the finite size of the nanocrystals. Upon the growth of the InP shell (dashed line), peak positions shift to higher angles, towards the positions of the bulk InP zinc blende

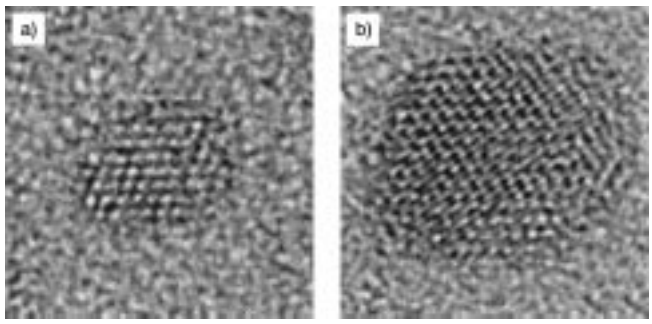

Figure 3. HRTEM images (8×8 nm) of a single InAs core nanocrystal (A), and an InAs/CdSe core/shell nanocrystal (B). Both nanocrystals are viewed in the [110] projection of the zinc blende structure.

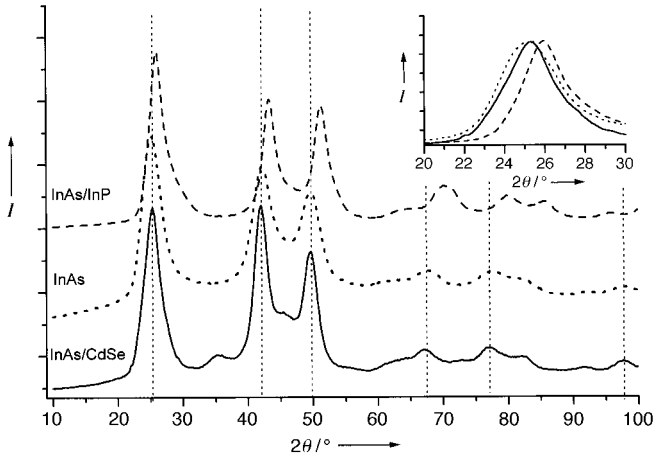

Figure 4. XRD patterns of InAs cores, 17 Å in radius (dotted line); InAs/InP core/shell with 25 Å shell thickness (dashed line); and InAs/CdSe core/shell with 14 Å shell thickness (solid line). The insert shows a zoom-in of the zinc blende (111) peak for the three samples, demonstrating the narrowing of the peaks upon shell growth.

peaks. In addition, substantial narrowing of the diffraction peaks is observed as demonstrated for the (111) peak shown in the insert of Figure 4. The narrowing results from an increase of the crystalline domain size, indicating that shell growth is epitaxial. For the CdSe shells (solid line), the peak positions do not shift as compared with the InAs core. This is consistent with the nearly zero lattice mismatch of InAs and zinc blende CdSe, indicating epitaxial growth for this case as well. The diffraction peaks also narrow upon shell growth for the same reason as in the case of the InP shell.

InAs/InP and InAs/CdSe core/shell nanocrystals are similar in many respects including the basic synthetic route for their preparation, the epitaxial growth mode as evidenced by the XRD patterns, and the red shift of the absorption spectra upon shell growth. Moreover, the conduction band offsets between the InAs core and these two shell materials, and thus the radial electron potentials, are similar.[7] However, the fluorescence quantum yield of these two core/shell nanocrystals is completely different. Upon growth of the InP shells the quantum yield is quenched, while upon growth of the CdSe shells it is substantially increased. To explain this marked difference, we calculated the energy of the lowest electron state for both core/shells using a model of a particle in a spherical potential well.[12] We found that the energy of this state in both cases is higher than the core/shell conduction

  1433-7851/99/3824-3693 $ 17.50+.50/0

band offset, and as a result, the electron wavefunction has substantial probability of presence at the outer surface. Thus, the quality of the outer surface in the core/shell nanocrystals, may have a profound effect on the quantum yield.

To test this hypothesis, we carried out two experiments that directly affect the outer surface. In Figure 5a, we present the fluorescence spectra of fresh and oxidized InAs/InP core/shells. After oxidation, the absorption of the core/shells hardly

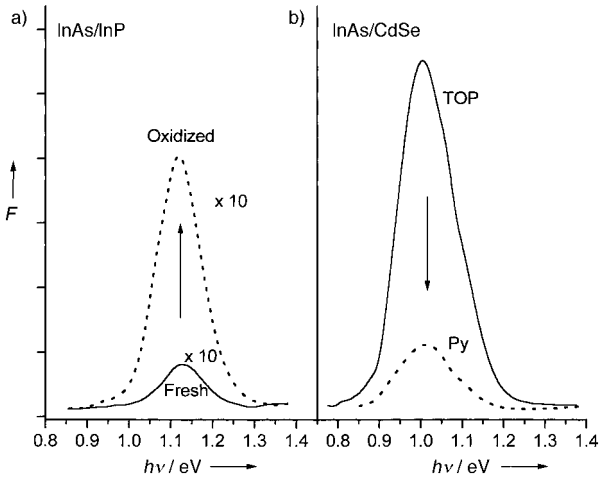

Figure 5. Outer surface effect in InAs/InP and in InAs/CdSe core/shell nanocrystals (core radius 17 Å, shell thickness 2 monolayers), detected by the fluorescence spectra. a) InAs/InP core/shells fresh (solid line), and oxidized (dotted line) in O_2-saturated toluene for four days. b) Fluorescence for InAs/CdSe core/shells capped by TOP (solid line), and by pyridine (dotted line). All the spectra were taken in the same conditions, and presented in the same fluorescence intensity scale, with the InAs/InP spectra multiplied by 10.

changed, but the fluorescence quantum yield increased by a factor of 6, up to the level of the fresh core. This directly demonstrates the importance of the outer surface for the InAs/InP core/shell fluorescence. A similar behavior was observed previously upon oxidation of InP nanocrystals.[13] In Figure 5b, we compare the fluorescence spectra of InAs/CdSe core/shells coated by trioctylphosphine (TOP), with another fraction of the same core/shells coated by pyridine. The quantum yield of the pyridine-coated nanocrystals is substantially quenched compared to the TOP-coated nanocrystals. The absorption of these samples was similar, and the quenching of the fluorescence can be directly assigned to the change of the outer surface.[4] The two experiments provide direct evidence for the importance of the outer surface in determining the fluorescence QY of these core/shell nanocrystals. For the InAs/CdSe core/shells, where the outer surface quality is high, we obtained a substantial enhancement of the fluorescence QY up to levels better than traditional organic IR dyes, and with improved photostability.

Experimental Section

A two-step synthesis route was used to prepare the core/shell nanocrystals. In the first step, InAs nanocrystals with controlled sizes between 10 – 40 Å in radius were synthesized by using a pyrolytic reaction of organometallic precursors, Tris(trimethylsilyl)arsenide and indium(III) chloride, in a liquid surfactant, trioctylphosphine (TOP).[14,15] The width of the size distribution of cores after this synthesis was on the order of 15 %. Before shell growth, we improved the size distribution of the cores to 10 %, using size-selective precipitation. In the second step, the shell was grown. InAs cores were dissolved in TOP (3 – 6 g) in a three-necked flask. Under a flow of argon on a Schlenk line, the nanocrystal solution was heated to 260 °C, and the InP shell precursor solution (indium(III)chloride and tris(trimethylsilyl)phosphane TOP solution), or CdSe shell precursor solution (dimethylcadmium and tributylphosphane selenide TOP solution) were introduced into the hot solution by dropwise addition. After addition was complete, the reaction mixture was cooled to room temperature. InAs/InP or InAs/CdSe core/shell nanocrystals passivated by TOP were obtained by precipitation using a mixture of methanol and toluene. The growth of cores and core/shells was monitored by UV/Vis spectroscopy of aliquots taken from the reaction flask.

UV/Vis absorption spectra were measured by using a Shimadzu UV-1601 or UV-3101pc spectrophotometer. Photoluminescence experiments were performed using a He-Ne laser (632 nm, output power: 3 mW, spot size: 3 mm) as the excitation source. The emission was collected at a right angle configuration, dispersed by a monochromator and detected by a liquid nitrogen cooled InGaAs diode with lock-in amplification. Relative quantum yield measurements were carried out by using solutions with identical optical densities at the excitation wavelength. X-ray photoelectron spectroscopy (XPS) were performed by using a Perkin-Elmer PHI-5600 ESCA system under $Al_{K\alpha}$ radiation at 200 W. High-resolution spectra of As_{3d} and In_{3d} were obtained at a pass energy of 11.74 eV with a resolution of 0.025 eV per step interval. Transmission electron microscopy (TEM) to determine the shell thickness was conducted by using a Philips CM-120 microscope or a JEOL-100CX microscope. HRTEM images were obtained by using a JEOL-JEM-2010 electron microscope operated at 200 kV. Powder X-ray diffraction (XRD) patterns were obtained on a Philips PW-1830/40 X-ray diffractometer with $Cu_{K\alpha}$ radiation.

Received: June 7, 1999
Revised version: August 19, 1999 [Z13524IE]
German version: *Angew. Chem.* **1999**, *111*, 3913 – 3916

Keywords: crystal growth · fluorescence spectroscopy · luminescence · nanostructures · semiconductors

[1] H. Weller, *Angew. Chem.* **1993**, *105*, 56; *Angew. Chem. Int. Ed. Engl.* **1993**, *32*, 41.
[2] A. P. Alivisatos, S*cience* **1996**, *271*, 933.
[3] A. Mews, A. Eychmüller, M. Giersig, D. Schoos, H. Weller, *J. Phys. Chem.* **1994**, *98*, 934.
[4] X. Peng, M. C. Schlamp, A. V. Kadavanich, A. P. Alivisatos, *J. Am. Chem. Soc.* **1997**, *119*, 7019.
[5] B. O. Dabbousi, J. Rodriguez-Viejo, F. V. Mikulec, J. R. Heine, H. Mattoussi, R. Ober, K. F. Jensen, M. G. Bawendi, *J. Phys. Chem. B* **1997**, *101*, 9463.
[6] M. Bruchez, M. Moronne, P. Gin, S. Weiss, A. P. Alivisatos, *Science* **1998**, *281*, 2013.
[7] S. Wei, A. Zunger, *Appl. Phys. Lett.* **1998**, *72*, 2011.
[8] J. Wickham, X. Peng, A. P. Alivisatos, personal communication.
[9] S. Tanuma, C. J. Powell, D. R. Penn, *Surf. Interface Anal.* **1991**, *17*, 927.
[10] J. E. Bowen Katari, V. L. Colvin, A. P. Alivisatos, *J. Phys. Chem.* **1994**, *98*, 4109.
[11] M. Leduc, C. Weisbuch, *Opt. Commun.* **1978**, *26,* 78.
[12] D. Schoos, A. Mews, A. Eychmüller, H. Weller, *Phys. Rev. B* **1994**, *49*, 17072.
[13] A. A. Guzelian, J. E. B. Katari, A. V. Kadavanich, U. Banin, K. Hamad, E. Juban, A. P. Alivisatos, R. H. Wolters, C. C. Arnold, J. R. Heath, *J. Phys. Chem.* **1996**, *100*, 7212.
[14] A. A. Guzelian, U. Banin, A. V. Kadavanich, X. Peng, A. P. Alivisatos, *Appl. Phys. Lett.* **1996**, *69*, 1432.
[15] X. Peng, J. Wickham, A. P. Alivisatos, *J. Am. Chem. Soc.* **1998**, *120*, 5343.

  1433-7851/99/3824-3694 $ 17.50+.50/0